

# Photoelastic and Numerical Models of the Fracture in the Multi – Layered Composites

Mieczysław Jaroniek<sup>1</sup>

<sup>1</sup> Department of Materials and Structures Strength, Technical University of Łódź, Poland

***ABSTRACT:** Advanced mechanical and structural applications require accurate assessment of the damage state of materials during the fabrications as well as during the service. Due to the complex nature of the internal structure of the material, composites including the layered composite often fail in a variety of modes. The failure modes very often are influenced by the local material properties that may develop in time under heat and pressure, local defect distribution, process induced residual stress, and other factors. Consider a laminate composite in plane stress conditions, multi-layered beam bonded to planes having shear modulus  $G_1$  and Poissons ratio  $\nu_1$  respectively, subjected to bending. The behaviour of the cracks depends on the cracks configuration, size, orientation, material properties, and loading characteristic. The fracture mechanics problem will be attacked using the photoelastic visualisation of the fracture events in a model structure. The proposed experimental method will developed fracture mechanics tools for a layered composite fracture problem.*

## INTRODUCTION

The development of the failure criterion for a particular application is very important for the predictions of the crack path and critical loads.

Recently, there has been a successful attempt to formulate problems of multiple cracks without any limitation. This attempt was concluded with the series of papers summarising the undertaken research for isotropic [2], an isotropic [4] and non-homogeneous class of problems [5] and [4].

Crack propagation in multi-layered composites of finite thickness is especially challenging and open field for investigation. Some results have been recently reported in [5]. The numerical calculations were carried out using the finite element programs ANSYS 5.4 and 5.6 [8]. Two different methods were used: solid modeling and direct generation.

## MATERIAL PROPERTIES

Material properties exert an influence on the stress distribution and concentration, damage process and load carrying capacity of elements. In the case

of elastic-plastic materials, a region of plastic strains originates in most heavily loaded cross-sections. In order to visualise the state of strains and stresses, some tests have been performed on the samples made of an "araldite"-type optically active epoxy resin (Ep-53), modified with softening agents in such a way that an elastic material has been obtained. Properties of the components of experimental model are given in Table 1.

TABLE 1: Mechanical properties of the experimental model components

Layer	Young's Modulus $E_i$ [MPa]	Poisson's ratio $\nu_i$ [1]	Photoelastic constants in terms of stresses $k_\sigma$ [MPa/fr]	Photoelastic constants in terms of strain $f_\epsilon$ [-/fr]
1	3450.0	0.35	1.68	$6.572 \cdot 10^{-4}$
2	1705.0	0.36	1.18	$9.412 \cdot 10^{-4}$
3	821.0	0.38	0.855	$14.31 \cdot 10^{-4}$
4	683.0	0.40	0.819	$16.79 \cdot 10^{-4}$

## EXPERIMENTAL RESULTS

The stress distribution in was determined using two methods: **Shear Stress Difference Procedure** (SDP – evaluation a complete stress state by means the isochromatics and the angles of the isoclines along the cuts) [3].

**Method of the characteristics** (the stress distribution were determined using the isochromatics only and the equations of equilibrium [8].

In a general case [7], the Cartesian components of stress:  $\sigma_x$ ,  $\sigma_y$  and  $\tau_{xy}$  in the neighbourhood of the crack tip are:

$$\begin{aligned}
 \sigma_x &= \frac{1}{\sqrt{2\pi r}} [K_I \cos \frac{\theta}{2} (1 - \sin \frac{\theta}{2} \sin \frac{3\theta}{2}) - K_{II} \sin \frac{\theta}{2} (2 + \cos \frac{\theta}{2} \cos \frac{3\theta}{2})] + \sigma_{ox} \\
 \sigma_y &= \frac{1}{\sqrt{2\pi r}} [K_I \cos \frac{\theta}{2} (1 + \sin \frac{\theta}{2} \sin \frac{3\theta}{2}) + K_{II} \sin \frac{\theta}{2} \cos \frac{\theta}{2} \cos \frac{3\theta}{2}] \\
 \tau_{xy} &= \frac{1}{\sqrt{2\pi r}} [K_I \sin \frac{\theta}{2} \cos \frac{\theta}{2} \cos \frac{3\theta}{2} + K_{II} \cos \frac{\theta}{2} (1 - \sin \frac{\theta}{2} \sin \frac{2\theta}{2})]
 \end{aligned} \tag{1}$$

From which:

$$\begin{aligned}
 (\sigma_1 - \sigma_2)^2 &= \frac{1}{2\pi r} [(K_I \sin \theta + 2K_{II} \cos \theta)^2 + (K_{II} \sin \theta)^2] - \\
 &- 2 \frac{\sigma_{ox}}{\sqrt{2\pi r}} \sin \frac{\theta}{2} [K_I \sin \theta (1 + 2 \cos \theta) + K_{II} (1 + 2 \cos^2 \theta + \cos \theta)] + \sigma_{ox}^2
 \end{aligned} \tag{2}$$

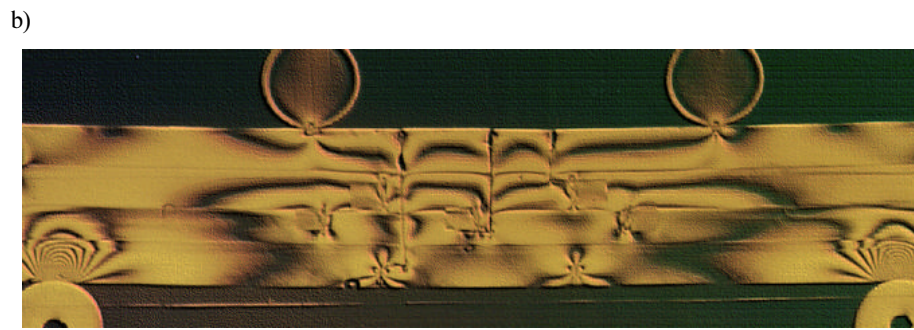
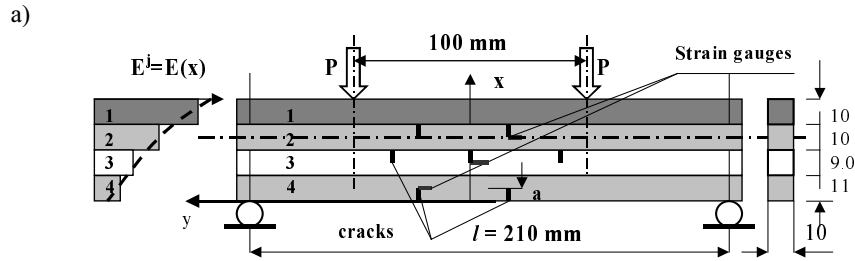


**Figure 1:** a) Four-layer beam with cracks. Photoelastic model under four point bending, the isochromatic patterns ( $\sigma_1 - \sigma_2$ ) distribution b) Initial loading ( $P = 20.0$  N). c)  $P = 50.0$  N - tension of layers 2, 3 and 4.

By inserting the values  $k_{\sigma} m_i = \sigma_1 - \sigma_2$  into (2) we obtain the isochromatic curves in polar coordinates ( $r, \theta$ ). For each isochromatic loop the position of maximum angle  $\theta_m$  corresponds to the maximum radius of the  $r_m$ . This principle can also be used in the mixed mode analysis [11] by employing information from two loops in the near field of the crack, if the far field stress component -  $\sigma_{ox}(\theta) = \text{const}$ . Differentiating Eq. 2 with respect to  $\theta$ , setting  $\theta = \theta_m$  and  $r = r_m$  and using Eq. ( $\partial \tau_m / \partial \theta_m = 0$ ) gives:

$$\begin{aligned}
g(K_I, K_{II}, \sigma_{ox}) &= \frac{1}{2\pi r} [K_I^2 \sin 2\Theta + 4K_I K_{II} \cos 2\Theta - 3K_{II}^2 \sin 2\Theta] - \\
&- 2 \frac{\sigma_{ox}}{\sqrt{2\pi r}} \sin \frac{\Theta}{2} \{ [K_I (\cos \Theta + 2 \cos 2\Theta) - K_{II} (2 \sin 2\Theta + \sin \Theta)] + \\
&+ \frac{1}{2} \cos \frac{\Theta}{2} [K_I (\sin \Theta + \sin 2\Theta) + K_{II} (2 + \cos 2\Theta + \cos \Theta)] \} \\
f(K_I, K_{II}, \sigma_{ox}) &= (\sigma_1 - \sigma_2)^2 - (k_\sigma \cdot m)^2 = 0
\end{aligned}$$

and

$$g(K_I, K_{II}, \sigma_{ox}) = \frac{\partial [(\sigma_1 - \sigma_2)^2]}{\partial \Theta_m} = 0 \quad (3)$$

Substituting the radii  $r_m$  and the angles  $\Theta_m$  from these two loops into a pair of equations of the form given in Eq. 3 gives two independent relations dependent on the parameters  $K_I$ ,  $K_{II}$  and  $\sigma_{ox}$ . The third equation is obtained by using Eq. 2. The three equations obtained in this way have the form

$$g_i(K_I, K_{II}, \sigma_{ox}) = 0, \quad g_j(K_I, K_{II}, \sigma_{ox}) = 0, \quad f_k(K_I, K_{II}, \sigma_{ox}) = 0 \quad (4)$$

In order to determine  $K_I$ ,  $K_{II}$  and  $\sigma_{ox}$  it is sufficient to select two arbitrary points  $r_i$ ,  $\Theta_i$  and apply the Newton-Raphson method to the solution of three simultaneous non-linear Eq. 4. The values  $K_C$  according to mixed mode of the fracture were obtained from

$$K_C = \sqrt{K_I^2 + K_{II}^2} \quad (5)$$

Example of the numerical results obtained from Eq. 4:

for  $m_1 = 12.5$ ,  $r_1 = 0.6$  m,  $\Theta_1 = 1.484$ ,  $r_2 = 10.45$  mm,  $\Theta_2 = 1.416$

$K_I^{(4)} = 0.14$  MPa $\sqrt{m}$ ,  $K_{II}^{(4)} = 1.05$  MPa $\sqrt{m}$ ,  $\sigma_{ox} = 0.039$  MPa,  $K_C^{(4)} = 1.05$  MPa $\sqrt{m}$

By inserting the values  $r_i$ ,  $\Theta_i$  in three selected arbitrary points into (2) we obtain three non-linear equations ( $i = 1, 2, 3$ )

$$f_i(K_I, K_{II}, \sigma_{ox}) = 0 \quad (6)$$

and apply the Newton-Raphson method to the solution we have  $K_I$ ,  $K_{II}$  and  $\sigma_{ox}$ . Example of the numerical results (shown in Figure 3) obtained from (6): for  $m_1 = 12.5$ ,  $r_1 = 0.72$  mm,  $\Theta_1 = 1.484$ ,  $m_2 = 8.0$ ,  $r_2 = 1.15$  mm,  $\Theta_2 = 1.375$ ,  $m_3 = 5.5$  mm,  $r_3 = 1.85$ ,  $\Theta_3 = 1.315$   
 $K_I^{(4)} = 0.702$  MPa $\sqrt{m}$ ,  $K_{II}^{(4)} = 1.043$  MPa $\sqrt{m}$ ,  $\sigma_{ox} = 0.152$  MPa,  $K_C^{(4)} = 1.257$  MPa $\sqrt{m}$

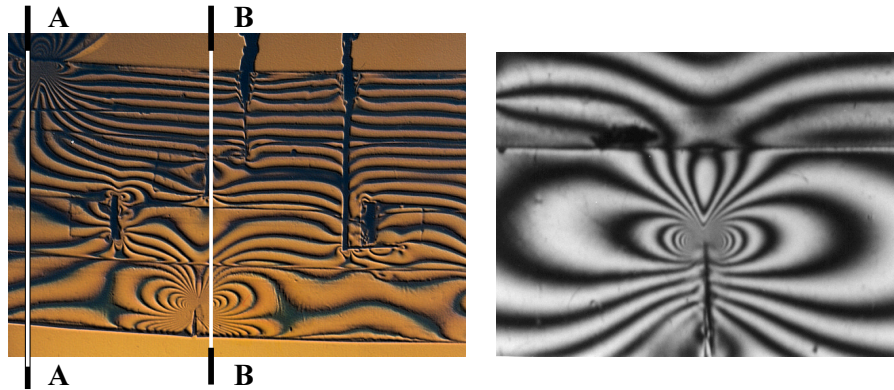


**Figure 2:** The isochromatic patterns ( $\sigma_1 - \sigma_2$ ) distribution according to the propagation of the crack obtained experimentally.

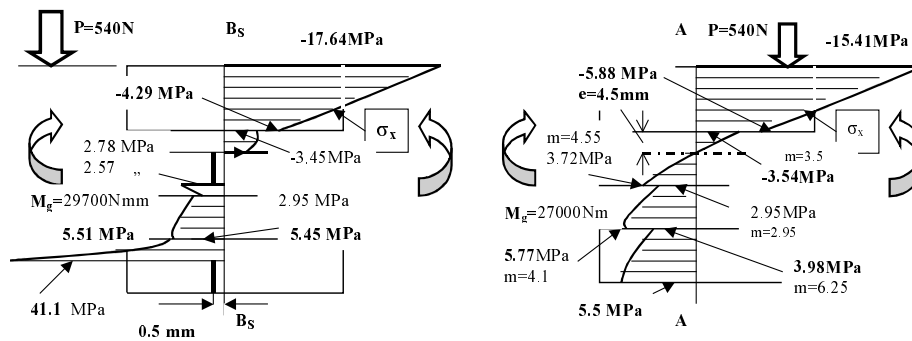


**Figure 3:** Distribution of stresses  $\sigma_x$  in cross sections A-A and B-B 0.5 mm with respect to crack obtained experimentally.

### NUMERICAL DETERMINATION OF STRESS DISTRIBUTION

The distribution of stresses and displacements has been calculated using the finite element method (FEM) [9]. Finite element calculations were performed in order to verify the experimentally observed the isochromatic distribution observe during cracks propagation. The geometry and materials of models were chosen to correspond to the actual specimens used in the experiments. The numerical calculations were carried out using the finite element program ANSYS 5.4 and by applying the substructure technique. For comparison the numerical (from FEM) and experimental isochromatic fringes ( $\sigma_1 - \sigma_2$ ), distribution was shown in Figure 3. A finite element mesh

of the model (used for numerical simulation) are presented in Fig.5 and the stresses  $\sigma_x$  are shown in Figures 6 and 7.

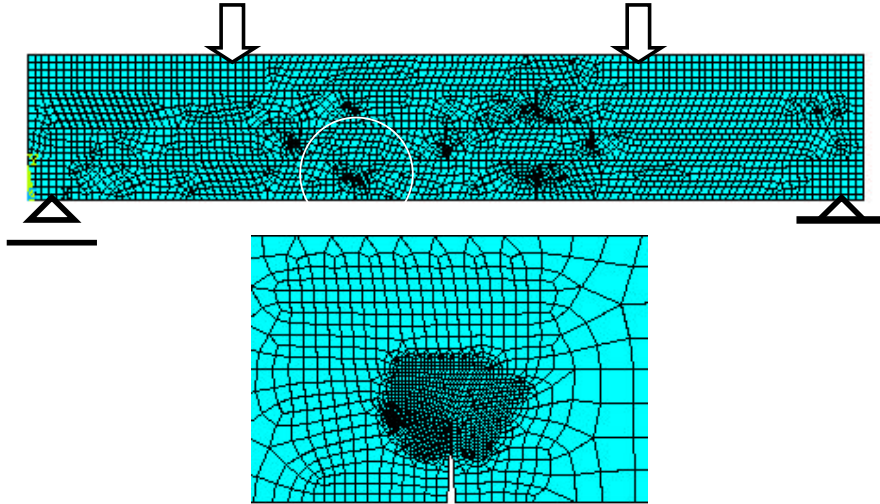


**Figure 4:** A finite element mesh of the model (for numerical simulation).

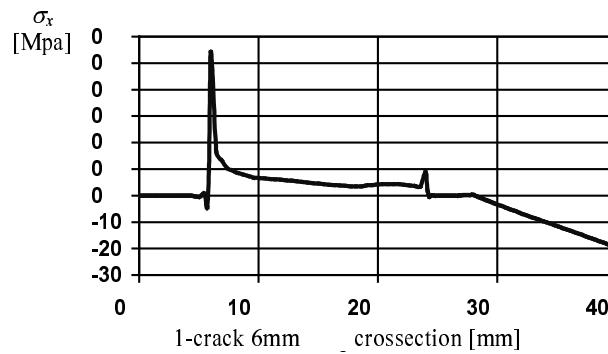


**Figure 5:** Numerical determination of stress distribution (Ansys 5.4). Distribution of the stresses  $\sigma_x$  along the crack.

The strain energy release rate  $G_C$  equal in this case to the Rice  $J$ -integral:

$$J = \int_s \left( \frac{1}{2} \sigma_{ij} \varepsilon_{ij} dx_2 - T_i^n \frac{\partial u_i}{\partial x_1} ds \right) \quad (7)$$

or from numerical calculation using the finite element method:

$$J = \sum_j \left\{ \frac{1}{2} \left[ \frac{1}{E_i} (\sigma_{yi}^2 - \sigma_{xi}^2) + \frac{\tau_{xyi}^2}{2G} \right] \cdot n_{1i} - \left[ \frac{\tau_{xyi}}{E_i} (\sigma_{xi} - \nu \sigma_{yi}) \cdot n_{2i} + (\tau_{xyi} n_{1i} + \sigma_{yi} n_{2i}) \frac{\Delta v_i}{\Delta x_i} \right] \right\} \cdot \Delta S_i \quad (8)$$

The values  $K_C$  according to the fracture in the 4-layer were determined from

$$K_C^{(i)} = \sqrt{E_i \cdot G_C} \quad (9)$$

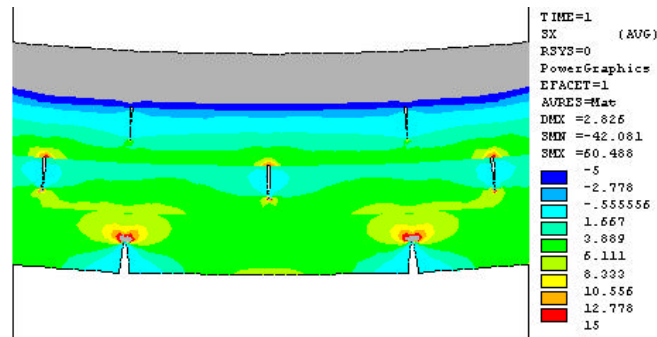
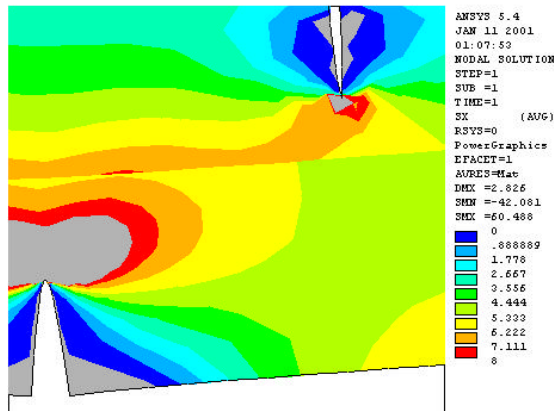


**Figure 6:** Numerical determination of stress distribution (Ansys 5.4). Distribution of the stresses  $\sigma_x$  (cracks length  $a = 6.0$  mm).

1)  $a = 6.0$  mm



2)  $a = 9.0$  mm

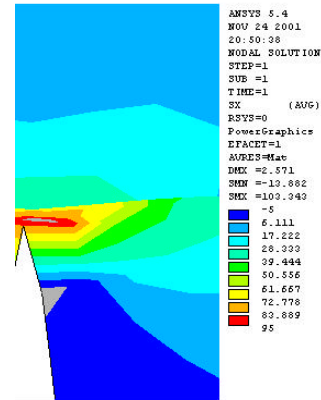


**Figure 7:** Numerical results. (Ansys 5.4). Distribution of the stresses  $\sigma_x$ , cracks length 1)  $a = 6.0$  mm and 2)  $a = 9.0$  mm, thickness of layers  $h = 10$  mm.

TABLE 2: Experimental and numerical results.  
Critical values  $K_{IC}^{(4)}$  according to the propagation of the crack.

Crack length $a$ [mm]	Critical force $P_{cr}$ [N]	Experimental results [MPa $\sqrt{m}$ ]				Numerical results	
		$K_I^{(4)}$	$K_{II}^{(4)}$	$K_C^{(4)}$	$\sigma_{ox}$ [MPa]	$G_C^{(4)}$ [MN/m]	$K_C^{(4)}$ [MPa $\sqrt{m}$ ]
6.0	265.0	1.177	0.8793	<b>1.419</b>	2.58	3.08	<b>1.45</b>
9.0	205.0	0.702	1.043	<b>1.257</b>	0.152	2.39	<b>1.28</b>
9.8	185.0	0.14	1.05	<b>1.05</b>	0.039	1.97	<b>1.16</b>

## CONCLUSIONS

Photoelasticity was shown to be promising method in stress analysis of beams with various number and orientation of cracks. It is possible to fabricate a model using various photoelastic materials to model multi-layered structure. Finite element calculations (FEM) were performed in order to verify the experimentally observed branching phenomenon and the isochromatic distribution observed during cracks propagation. The agreement between the finite element method predicted isochromatics-fringe patterns distribution and those determined photoelastically was found to be within 3÷5 percent.

## REFERENCES

1. Cherepanov G. P. (1979) *Mechanics of Brittle Fracture*. Mc Graw - Hill, New York.
2. Cook T. S. and Erdogan F. (1972) In: *International Journal of Engineering Science*, **10**, 677.
3. Frocht M. M. (1960) *Photoelasticity*, John Wiley, New York.
4. Gupta A. G., A (1973) *International Journal of Solids and Structures*, **36**, 1845.
5. Hilton P. D. and Sin G. C. (1971) *International Journal of Solids and Structures*, **7**, 913.
6. Neimitz A. (1998) *Mechanics of fracture*. (in Polish) PWN, Warsaw.
7. Sanford R. J. and Dally J. (1979) *Engineering Fracture Mechanics*, **2**, 621.
8. Szczepiński W. (1961) *Archives of Applied Mechanics* **5**.
9. User's Guide ANSYS (1999) 5.4, 5.6, Ansys, Inc., Huston, USA.
10. Zienkiewicz O. C. (1971) *The Finite Element Method in Engineering Science*. Mc Graw - Hill, London, New York.